culation two to three times as long as Epo (Table 1) (*33*). These data show that SEP both is a potent effector of red blood cell formation and has prolonged duration of action in vivo.

It is a long-standing goal of chemical protein synthesis to generate proteins with novel properties (*13, 14*). In the work reported here, we demonstrate that it is now possible to design and produce polymer-modified proteins that have full biological potency and increased in vivo lifetimes. The ability to construct homogeneous protein therapeutics such as SEP enables the systematic exploration of structure-function relationships, and consequent fine-tuning of the biological properties of the protein of interest. Such molecules are not accessible with current recombinant DNA–based protein expression or by post-expression protein modification with polyethylene glycol (*6–9, 34, 35*).

Chemical synthesis is free of inherent biological contamination (nucleic acids, viruses, prion proteins, etc.). It uses readily available building blocks (synthetic peptides, precision-length polymers) and is scalable. Also, it enables complete control over design, incorporation of noncoded elements, and the precision modification of the protein of interest. Chemical protein synthesis thus addresses the known shortcomings of existing protein therapeutics and provides a tool for the rapid and effective development of new protein therapeutic leads.

References and Notes

1. M. N. Fukuda, H. Sasaki, L. Lopez, M. Fukuda, *Blood* **73**, 84 (1989).
2. J. L. Spivak, B. B. Hogans, *Blood* **73**, 90 (1989).
3. T. Misaizu *et al.*, *Blood* **86**, 4097 (1995).
4. J. C. Egrie, J. K. Browne, *Br. J. Cancer* **84** (suppl. 1), 3 (2001).
5. Glycoforms are proteins of identical protein backbone that carry sugars of varying number, complexity, and charge.
6. P. Bailon *et al.*, *Bioconjug. Chem.* **12**, 195 (2001).
7. G. Morstyn, M. A. Foote, T. Walker, G. Molineux, *Acta Haematol.* **105**, 151 (2001).
8. J. F. Eliason, *BioDrugs* **15**, 705 (2001).
9. F. M. Veronese, *Biomaterials* **22**, 405 (2001).
10. M. Schnölzer, S. B. H. Kent, *Science* **256**, 221 (1992).
11. P. E. Dawson, T. W. Muir, I. Clark-Lewis, S. B. H. Kent, *Science* **266**, 776 (1994).
12. K. Rose, *J. Am. Chem. Soc.* **116**, 30 (1994).
13. P. E. Dawson, S. B. H. Kent, *Annu. Rev. Biochem.* **69**, 923 (2000).
14. G. G. Kochendoerfer, *Curr. Opin. Drug Discov. Dev.* **4**, 205 (2001).
15. K. Rose, J. Vizzavona, *J. Am. Chem. Soc.* **121**, 7034 (1999).
16. K. Jacobs *et al.*, *Nature* **313**, 806 (1985).
17. P. H. Lai, R. Everett, F. F. Wang, T. Arakawa, E. Goldwasser, *J. Biol. Chem.* **261**, 3116 (1986).
18. Analogs that carried more or fewer negative charges on the precision polymer moiety or that had a lower-molecular-weight precision polymer attached exhibited significantly less potency and shorter duration of action when tested at similar doses (G. Kochendoerfer *et al.*, unpublished observation).
19. M. Schnölzer, P. Alewood, A. Jones, D. Alewood, S. B. H. Kent, *Int. J. Pept. Protein Res.* **40**, 180 (1992).
20. For a description of amino acid sequences and synthetic procedures, see supporting material on *Science* Online.
21. This novel stratagem was dictated by the asymmetric distribution of the four Cys residues in the target 166-residue polypeptide chain, and necessitated differential protection of the other Cys side chains present at the alkylation step: Cys^{161}(picolyl) and Cys^{33} (acetamidomethyl).
22. V. P. Saxena, D. B. Wetlaufer, *Biochemistry* **9**, 5015 (1970).
23. As designed, SEP had an artificially high apparent molecular mass. Measurement under nondenaturing conditions by size-exclusion chromatography gave an apparent effective hydrodynamic size of ~330 kD. These data show that the precision polymer increases the apparent molecular mass of SEP, presumably because of preferential hydration of the polymer portion of SEP.
24. SEP had a calculated mass of 50,821 daltons (average isotope composition).
25. F. Mao, unpublished observations.
26. J. M. Davis, T. Arakawa, T. W. Strickland, D. A. Yphantis, *Biochemistry* **26**, 2633 (1987).
27. This is in stark contrast to both typical glycoproteins, such as Epo, and typical polymer-modified proteins, all of which are highly heterogeneous in both polymer composition and sites of attachment.
28. N. Komatsu *et al.*, *Blood* **82**, 456 (1993).
29. Average SEP [median effective dose (ED_{50}) = 1.3 ng/ml] has activity comparable to Epo (ED_{50} = 1.1 ng/ml) within the uncertainty of the experiment on the basis of protein backbone concentrations.
30. M. Yamasaki, M. Asano, M. Okabe, M. Morimoto, Y. Yokoo, *J. Biochem. (Tokyo)* **115**, 814 (1994).
31. Y. Tsutsumi *et al.*, *Jpn. J. Cancer Res.* **85**, 9 (1994).
32. R. Clark *et al.*, *J. Biol. Chem.* **271**, 21969 (1996).
33. This effect is most likely due to reduced renal clearance. In addition, absence of glycosylation prevents specific clearance of SEP by the asialoglycoprotein receptor that is predominantly responsible for the clearance of Epo (*1, 2*).
34. S. T. Cload, D. R. Liu, W. A. Froland, P. G. Schultz, *Chem. Biol.* **3**, 1033 (1996).
35. L. Wang, P. G. Schultz, *Chem. Biol.* **8**, 883 (2001).

36. We thank Midwest Biotech for the large-scale custom synthesis of Boc-Cys(Pic)-OH, S. J. Phillips for the coordination of the in vivo studies, and C. E. Green, Y. Freund, and L. Olson for help with the PK study.

Supporting Online Material

www.sciencemag.org/cgi/content/full/299/5608/884/DC1

Materials and Methods

4 October 2002; accepted 2 January 2003

Myc-Induced T Cell Leukemia in Transgenic Zebrafish

David M. Langenau,[1] David Traver,[2] Adolfo A. Ferrando,[1] Jeffery L. Kutok,[3] Jon C. Aster,[3] John P. Kanki,[1] Shuo Lin,[4] Ed Prochownik,[5] Nikolaus S. Trede,[2] Leonard I. Zon,[2] A. Thomas Look[1]*

The zebrafish is an attractive model organism for studying cancer development because of its genetic accessibility. Here we describe the induction of clonally derived T cell acute lymphoblastic leukemia in transgenic zebrafish expressing mouse c-*myc* under control of the zebrafish *Rag2* promoter. Visualization of leukemic cells expressing a chimeric transgene encoding Myc fused to green fluorescent protein (GFP) revealed that leukemias arose in the thymus, spread locally into gill arches and retro-orbital soft tissue, and then disseminated into skeletal muscle and abdominal organs. Leukemic cells homed back to the thymus in irradiated fish transplanted with GFP-labeled leukemic lymphoblasts. This transgenic model provides a platform for drug screens and for genetic screens aimed at identifying mutations that suppress or enhance c-*myc*–induced carcinogenesis.

The zebrafish (*Danio rerio*) is a potentially valuable vertebrate system in which to elucidate novel molecular pathways of oncogenesis. In particular, this model organism develops an array of benign and malignant tumors resembling those in humans (*1, 2*) and is amenable to large-scale forward genetic screens that could be targeted to conserved cancer pathways (*3, 4*). However, it has not been possible to establish stable lines of transgenic tumor-bearing fish. Here we report the induction of T cell leukemia in zebrafish, using mouse c-*myc* (*mMyc*) and chimeric *EGFP-mMyc* transgenes (*5*) under control of the zebrafish *Rag2* promoter (*zRag2*), which targets gene expression specifically to lymphoid cells (*6*). This transgenic strategy is based on the demonstrated role of *MYC* in the pathogenesis of human T and B cell leukemias and lymphomas and its ability to induce T and B lymphoid malignancies when aberrantly expressed in transgenic mice [reviewed in (*7, 8*)].

We microinjected wild-type zebrafish embryos with the *zRag2-mMyc* or *zRag2-EGFP-mMyc* transgene at the one-cell stage of development (*9*), generating F_0 founder fish mosaic for expression of the transgene (*10*). Of 215 mosaic F_0 zebrafish embryos injected

[1]Department of Pediatric Oncology, Dana-Farber Cancer Institute, Harvard Medical School, Boston, MA 02115, USA. [2]Division of Hematology/Oncology, Children's Hospital Boston, Harvard Medical School, Boston, MA 02115, USA. [3]Department of Pathology, Brigham and Women's Hospital, Boston, MA 02115, USA. [4]Department of Molecular, Cell and Developmental Biology, University of California, Los Angeles, CA 90095, USA. [5]Division of Hematology/Oncology, Children's Hospital of Pittsburgh, Pittsburgh, PA 15213, USA.

*To whom correspondence should be addressed. E-mail: thomas_look@dfci.harvard.edu

with *zRag2-mMyc*, 11 (5%) developed tumors, as did 7 (6%) of 122 injected with *zRag2-EGFP-mMyc*. These results are similar to the proportion of embryos expressing green fluorescent protein (GFP) in developing thymocytes after injection of the control *zRag2-GFP* reporter construct, suggesting that cancer develops in nearly every mosaic fish whose lymphoid progenitors carry a functional *mMyc* transgene. The mean latencies of tumor development in *zRag2-mMyc*$^+$ and *zRag2-EGFP-mMyc*$^+$ fish were 44 and 52 days (range, 30 to 131 days), respectively.

The affected zebrafish had distended abdominal cavities and splayed eyes due to retro-orbital infiltration by malignant cells (compare Fig. 1, A and B, with Fig. 1, C and D). Some fish had growths protruding from under the operculum adjacent to the thymus (fig. S1, A and B), whereas some had tumors at the base of the pectoral fin (Fig. 1, C and D). Many of the fish showed extensive subcutaneous infiltration by transformed cells (Fig. 1F), resulting in progressive pallor.

To establish the extent of leukemic cell infiltration, we studied tissue sections from seven diseased fish. Lymphoblasts almost completely effaced the kidney marrow [the site of definitive hematopoiesis in the fish (Fig. 1, G and H)] and were found between the fibers of skeletal muscle (fig. S1, E and F). Leukemic cell invasion was also observed in the gut, gills, and fins, and it was especially prominent in the region adjacent to the olfactory bulb. Although zebrafish *Rag* genes are expressed at the apical surface of the olfactory placode (*6, 11*), malignant cells in the olfactory region did not express α-keratin and exhibited lymphoblast morphology, demonstrating that they were lymphoid and not epithelial in origin.

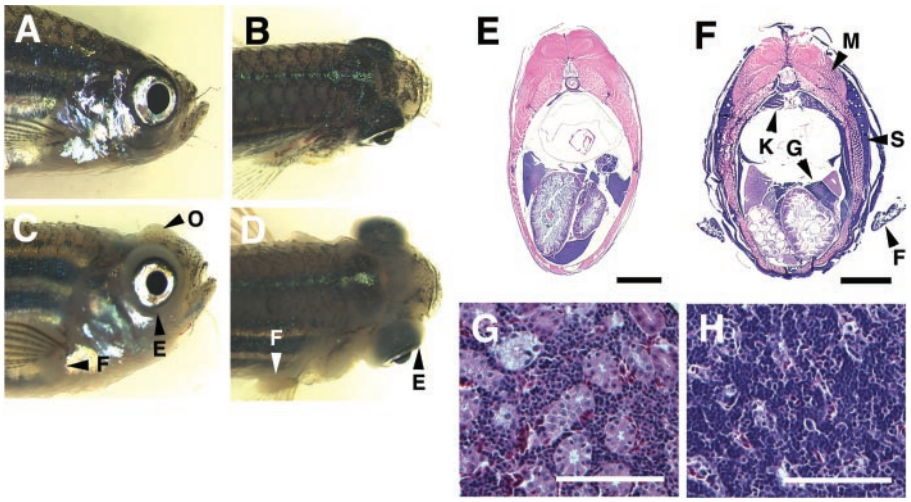

Fig. 1. External and histological features of leukemic *zRag2-mMyc* F_0 mosaic fish. (**A** and **B**) Wild-type fish and (**C** and **D**) *zRag2-EGFP-mMyc* fish with leukemic infiltration into the retro-orbital soft tissue, olfactory region, and pectoral fins. Transverse sections of (**E** and **G**) wild-type fish and (**F** and **H**) leukemic fish with massive infiltration of lymphoblasts throughout the body [(E) and (F)] and into the kidney [(G) and (H)]. E, eye; F, fin; G, gut; K, kidney; M, muscle; O, olfactory region; and S, skin. Arrowheads indicate sites of leukemic cells. Scale bars in (E) and (F), 1 mm; scale bars in (G) and (H), 100 μm.

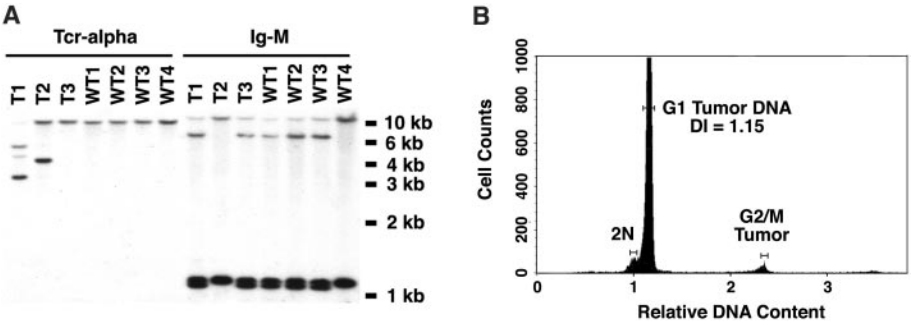

Fig. 2. Clonality of mMyc-induced leukemias. (**A**) Southern analysis of the *zTcr*-α and *zIgM* constant regions in leukemic (T1 through T3) and wild-type (WT1 through WT4) fish. The presence of either two or four restriction fragments hybridizing to the *zIgM* probe results from a Bgl II polymorphic site within the gene, not gene rearrangement. (**B**) DNA content of leukemic cells from a *zRag2-EGFP-mMyc* fish, as measured by flow cytometry. The DNA index (DI) of 1.15 for G_1-phase leukemic cells indicates clonal aneuploidy. 2N, DNA content of the normal diploid zebrafish genome. Bars indicate the postion of modal DNA content peaks corresponding to the indicated G_1 or G_2/M cell populations.

To analyze the gene expression patterns in transformed lymphoblasts, we applied RNA in situ hybridization to paraffin-embedded sections from seven leukemic F_0 fish, testing for expression of the T cell–specific gene *zLck*, the B cell–specific immunoglobulin heavy-chain (*zIgM*) and light-chain (*zIgLC*) genes (*12*), the early lymphoid genes *zRag1* and *zRag2*, and *mMyc*. Each of the leukemias expressed *mMyc* (fig. S3, A and E), *zRag2* (fig. S3, B and F), *zRag1* (*13*), and *zLck* (fig. S3, C and G), but not *zIgM* or *zIgLC*, confirming expression of the transgene and the derivation of these leukemias from cells of the T lymphoid lineage.

We further investigated the clonality and lineage of the lymphoblasts by Southern blot analysis of restriction enzyme–digested leukemic cell DNAs, using radiolabeled probes for *zTcr*-α (*12*) and *zIgM* constant regions. Of the three leukemias analyzed, one had monoclonal and one had oligoclonal *zTcr*-α gene rearrangements (Fig. 2A). The third showed a germ line *zTcr*-α configuration, but very strong *zLck* RNA expression, verifying the thymic origin of the lymphoblasts and suggesting that transformed thymocytes in this fish were developmentally arrested at a stage before *zTcr*-α gene rearrangement. None of the leukemias had rearranged *zIgM* genes. In addition, flow cytometric measurements of the DNA content of tumor cells from a *zRag2-EGFP-mMyc* fish showed that this Myc-induced tumor was clonally aneuploid (Fig. 2B). Taken together, these data indicate that Myc-induced leukemias in the zebrafish represent the clonal expansion of transformed T lymphocyte precursors and suggest that additional mutations are needed to produce the malignant phenotype.

To quantify the extent of leukemic cell infiltration of the kidney and spleen, we analyzed hematopoietic cells from these tissues by fluorescence-activated cell sorting (FACS) (*14*). In wild-type zebrafish, the kidney (n = 7) contained (8.4 ± 3.7) × 10^5 (mean ± SD) blood cells, and the spleen (n = 6) contained (8.2 ± 6.3) × 10^4 blood cells; these wild-type values were about one-sixth that of leukemic fish [kidney (n = 5), (4.95 ± 3.3) × 10^6 blood cells; spleen (n = 4), (4.64 ± 1.5) × 10^5 blood cells]. The leukemic blasts comprised ~87% of the kidney marrow cells and had a granularity similar to that of normal lymphocytes (y axis in Fig. 3), although they were slightly larger in size (x axis in Fig. 3). This analysis of the kidney marrow, the equivalent of mammalian bone marrow (*15–17*), supports the histopathological classification of these Myc-induced cancers as T cell acute leukemia rather than disseminated lymphoma, in which the blast cells account for <30% of the total cells in the marrow.

To assess the transplantability of zebrafish leukemic cells, we first injected the *zRag2-mMyc* transgene into fertilized eggs from a stable transgenic *zRag2-GFP* line, so that the lymphoblasts would be GFP positive when leukemia developed. GFP-positive lymphoblasts from a leukemic 62-day-old fish were then transplanted intraperitoneally into eight irradiated wild-type adult zebrafish. Leukemic cells were apparent at the site of transplantation within 7 days after injection (Fig. 4A) and had begun to spread throughout the peritoneal cavity within 14 days after injection (Fig. 4B). Lymphoblast homing to the thymus occurred relatively early in the disease process (fig. S6B), with GFP-positive cells becoming evident at this site in one fish within 14 days after injection and in six fish within 26 days after injection. There was also prominent leukemic cell infiltration into the region adjacent to the olfactory bulb in two fish within 14 days after injection and in all eight within 26 days after injection (fig. S6, C and D). These experiments establish the transplantability of Myc-induced leukemias in zebrafish, indicate that the disseminated spread of leukemic cells proceeds along anatomically defined pathways, and suggest that the region adjacent to the olfactory bulb is a preferred site for the homing of immature T cells.

The power of the zebrafish model lies in its ability to accommodate "forward-genetic" screens to identify modifier genes that influence the development of Myc-induced leukemia, an application requiring a stable transgenic zebrafish line that expresses the *mMyc* transgene. Thus, mosaic *zRag2-EGFP-mMyc* F_0 fish injected as single-cell embryos were mated, and the F_1 offspring of one fish developed leukemia with a mean latency of 32 days (range of 21 to 44 days). GFP fluorescence was readily detectable in the thymic lymphoblasts of these fish (Fig. 4, D through F), demonstrating germline transmission and expression of the chimeric transgene.

The rapid onset of leukemia after germline transmission of the transgene made it necessary to propagate this stable line by in vitro fertilization (IVF). Hence, we killed 90-day-old leukemic males and used their sperm to fertilize eggs from normal females. The resultant progeny showed expansion of GFP-positive leukemic cells from the thymus by 1 month of age. Technology to render the expression of transgenic myc alleles that are regulatable with estrogen has been developed for in vivo use in the mouse (*18*), and we are currently testing this approach for its capacity to generate large numbers of transgenic fish for further genetic manipulations, thus eliminating the need for IVF procedures.

Modifier screens in the mouse have identified retrovirally activated genes that accelerate Myc-induced oncogenesis (*19*), and breeding studies with genetically manipulated mice have identified other critical interact-

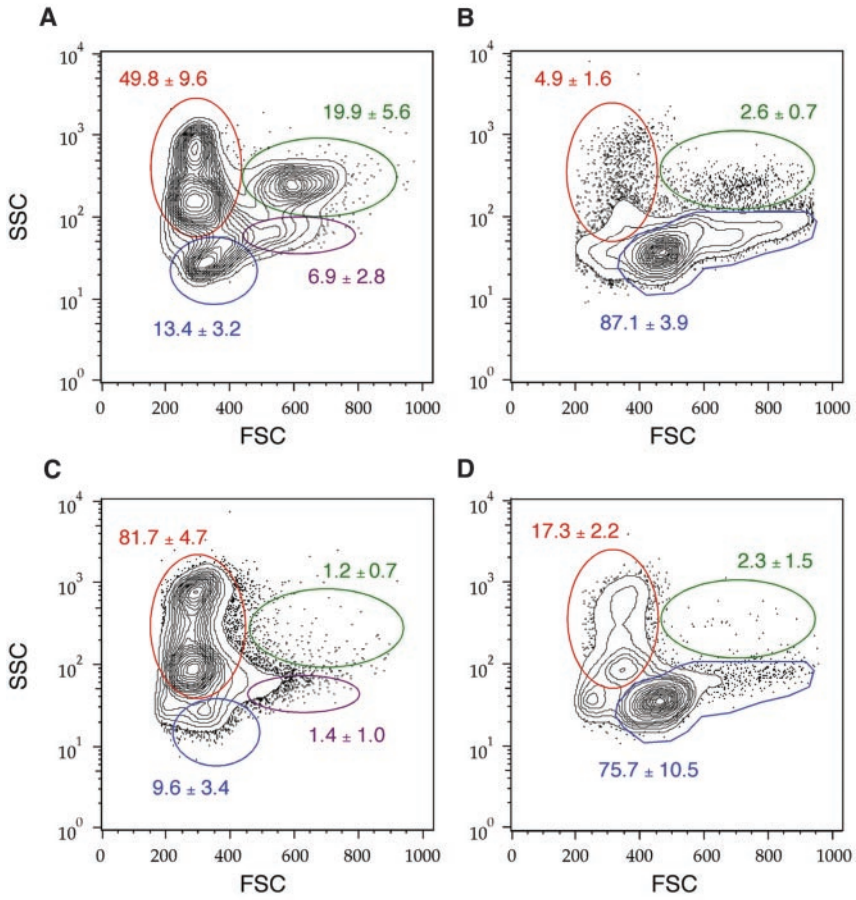

Fig. 3. FACS analysis of cells from kidney (top) and spleen (bottom) from (**A** and **C**) wild-type samples and (**B** and **D**) leukemic fish. Gated populations are as follows: erythrocytes (red), lymphocytes (blue), granulocytes and monocytes (green), and blood cell precursors in wild-type samples (purple). Populations of cells within each gate are described as mean percentages of total cells (±1 SD). Cell size is represented by forward scatter (FSC), and granularity is represented by side scatter (SSC).

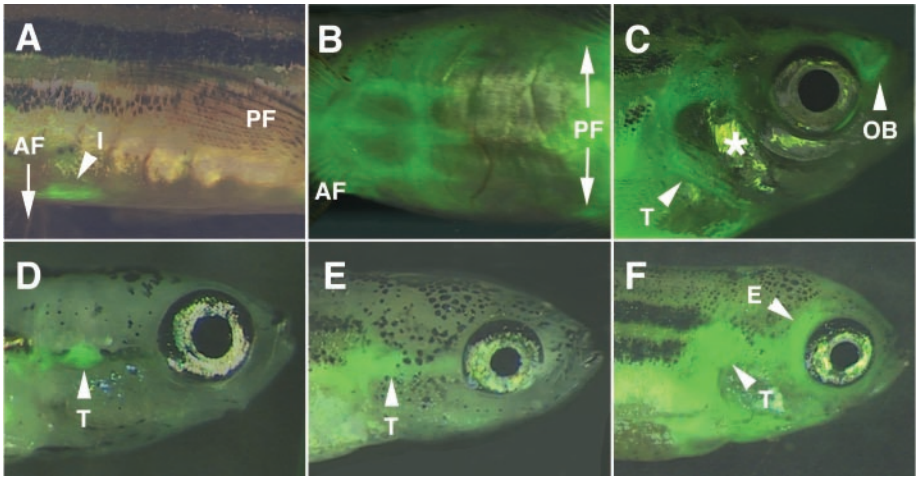

Fig. 4. Transplantability of zebrafish leukemias and germline transmission of *zRag2-EGFP-mMyc*. GFP-positive leukemic cells transplanted into sublethally irradiated adult fish were detected (**A**) at the site of injection into the peritoneal cavity at 14 days after injection, (**B**) in the peritoneal cavity at 24 days after injection, and (**C**) in the head region at 24 days after injection. After germline transmission of the *zRag2-EGFP-mMyc* transgene, GFP-positive leukemia progressed from (**D**) thymic enlargement, to (**E**) local infiltration of leukemic cells outside the thymus, to (**F**) extensive infiltration of the head. All panels are oriented with anterior to the right [lateral view, dorsal on top in (A) and (C) through (F) and ventral view in (B)]. AF, anal fin; E, eye; I, site of injection; OB, olfactory bulb; PF, pectoral fin; and T, thymic masses. Arrowheads indicate accumulations of leukemic cells. Autofluorescence is indicated with an asterisk.

ing oncogenes and tumor suppressors (*20, 21*). More recent studies in murine models have exploited tissue-specific, regulatable expression of myc alleles to show that myc expression is essential not only for establishment of the leukemic phenotype, but also for maintenance of the malignant phenotype (*22, 23*). Despite these advances, it has been difficult to conduct unbiased screens in the mouse to identify modifier genes whose inactivation delays or prevents the ability of Myc to generate a malignant phenotype. This obstacle could be overcome by conducting genomewide zebrafish screens for germline mutations induced by either ethylnitrosourea or retroviral integration. Such strategies would also be especially attractive for identifying tumor suppressor genes, as the mutant fish would carry inactivating mutations of single tumor suppressor alleles throughout development, increasing the likelihood of acquiring inactivating mutations or deletions affecting both alleles of the same gene. Such mutations may shed new light on the molecular mechanisms that drive T cell leukemia and other human cancers to which Myc has been linked (*24*). Others have demonstrated the utility of living zebrafish as subjects of screens for small molecules that perturb normal development (*25, 26*). Thus, our transgenic zebrafish model may also provide the opportunity to conduct large-scale screens for new drugs for the prevention and treatment of leukemia.

References and Notes

1. L. G. Beckwith, J. L. Moore, G. S. Tsao-Wu, J. C. Harshbarger, K. C. Cheng, *Lab. Invest.* **80**, 379 (2000).
2. J. F. Amatruda, J. L. Shepard, H. M. Stern, L. I. Zon, *Cancer Cell* **1**, 229 (2002).
3. W. Driever *et al.*, *Development* **123**, 37 (1996).
4. P. Haffter *et al.*, *Development* **123**, 1 (1996).
5. X. Yin *et al.*, *Oncogene* **20**, 4650 (2001).
6. J. R. Jessen, T. N. Jessen, S. S. Vogel, S. Lin, *Genesis* **29**, 156 (2001).
7. A. T. Look, in *The Genetic Basis of Human Disease*, B. Vogelstein, K. W. Kinzler, Eds. (McGraw-Hill, New York, 1998), chap. 5.
8. J. M. Adams, A. W. Harris, A. Strasser, S. Ogilvy, S. Cory, *Oncogene* **18**, 5268 (1999).
9. Materials and methods are available as supporting material on *Science* Online.
10. G. W. Stuart, J. V. McMurray, M. Westerfield, *Development* **103**, 403 (1988).
11. J. R. Jessen, C. E. Willett, S. Lin, *Nature Genet.* **23**, 16 (1999).
12. R. N. Haire, J. P. Rast, R. T. Litman, G. W. Litman, *Immunogenetics* **51**, 915 (2000).
13. D. M. Langenau *et al.*, data not shown.
14. D. Traver, L. I. Zon, in preparation.
15. K. Hsu, J. P. Kanki, A. T. Look, *Curr. Opin. Haematol.* **81**, 245 (2001).
16. C. M. Bennett *et al.*, *Blood* **98**, 643 (2001).
17. C. Thisse, L. I. Zon, *Science* **295**, 457 (2002).
18. S. Pelengaris, T. Littlewood, M. Khan, G. Elia, G. Evan, *Mol. Cell* **3**, 565 (1999).
19. H. Mikkers *et al.*, *Nature Genet.* **32**, 153 (2002).
20. X. Wu, P. P. Pandolfi, *Trends Cell Biol.* **11**, S2 (2001).
21. T. Van Dyke, T. Jacks, *Cell* **108**, 135 (2002).
22. M. Jain *et al.*, *Science* **297**, 102 (2002).
23. S. Pelengaris, M. Khan, G. I. Evan, *Cell* **109**, 321 (2002).
24. S. Pelengaris, M. Khan, G. Evan, *Nature Rev. Cancer* **2**, 764 (2002).
25. R. T. Peterson, B. A. Link, J. E. Dowling, S. L. Schreiber, *Proc. Natl. Acad. Sci. U.S.A.* **97**, 12965 (2000).
26. R. T. Peterson, J. D. Mably, J. N. Chen, M. C. Fishman, *Curr. Biol.* **11**, 1481 (2001).

27. We thank Y. Yang and M. Loda for paraffin sectioning and in situ analysis; J. Gilbert for editorial review; R. DePinho for the mouse *myc* cDNA; A. Winzeler for help with irradiation protocols; J. Morris for help with in vitro fertilization protocols; J. Vinokur, G. Kourkoulis, and W. Saganic for fish care and husbandry; and D. Dodson for manuscript preparation. Supported by NIH grants CA-68484 (A.T.L.) and CA-06516 (J.L.K. and J.C.A.). D.M.L. is an NSF predoctoral fellow, D.T. is supported by the Irvington Institute for Immunological Research, and A.A.F. is a fellow of the Leukemia and Lymphoma Society.

Supporting Online Material

www.sciencemag.org/cgi/content/full/299/5608/887/DC1
Materials and Methods
Supporting Online Text
Figs. S1 to S6
References and Notes

8 November 2002; accepted 8 January 2003

Angiogenesis-Independent Endothelial Protection of Liver: Role of VEGFR-1

Jennifer LeCouter,[1] Dirk R. Moritz,[1]* Bing Li,[2] Gail Lewis Phillips,[1] Xiao Huan Liang,[1] Hans-Peter Gerber,[1] Kenneth J. Hillan,[3] Napoleone Ferrara[1]†

The vascular endothelium was once thought to function primarily in nutrient and oxygen delivery, but recent evidence suggests that it may play a broader role in tissue homeostasis. To explore the role of sinusoidal endothelial cells (LSECs) in the adult liver, we studied the effects of vascular endothelial growth factor (VEGF) receptor activation on mouse hepatocyte growth. Delivery of VEGF-A increased liver mass in mice but did not stimulate growth of hepatocytes in vitro, unless LSECs were also present in the culture. Hepatocyte growth factor (HGF) was identified as one of the LSEC-derived paracrine mediators promoting hepatocyte growth. Selective activation of VEGF receptor–1 (VEGFR-1) stimulated hepatocyte but not endothelial proliferation in vivo and reduced liver damage in mice exposed to a hepatotoxin. Thus, VEGFR-1 agonists may have therapeutic potential for preservation of organ function in certain liver disorders.

The vascular endothelium is a highly versatile system and, in addition to its well-established function of nutrient and gas exchange between tissues and blood, it plays multiple homeostatic roles (*1*). Furthermore, the endothelium has an inductive effect on liver (*2*) and pancreas (*3*) development before the establishment of a blood flow. Vascular endothelial growth factor–A (VEGF-A) (*4*), a major regulator of normal and pathological angiogenesis, binds to two tyrosine kinase receptors, VEGFR-1 (Flt-1) (*5*) and VEGFR-2 (KDR/Flk-1) (*6, 7*). VEGFR-2 is the major mediator of the mitogenic, angiogenic, and permeability-enhancing effects of VEGF-A (*8*). However, many conflicting reports about the function of VEGFR-1 exist. This receptor has been implicated in the inhibition of VEGF-dependent endothelial mitogenesis and chemotaxis by several mechanisms (*9–11*). Other studies have shown that VEGFR-1 mediates monocyte chemotaxis (*12*), recruitment of endothelial cell progenitors (*13*), and survival of hematopoietic stem cells (*14*). VEGFR-1 activation also has been reported to result in collateral vessel growth through recruitment of bone marrow–derived cells (*15*). Thus, the importance of VEGFR-1 signaling in the vascular endothelium is largely unclear.

We sought to investigate the effects of VEGFR activation on parenchymal cell proliferation and survival. To achieve sustained systemic levels of VEGF, we injected Chinese hamster ovary (CHO) cells expressing $VEGF_{165}$ or control CHO cells into the legs of nude mice (*16*). We observed substantially increased liver sizes in the CHO-VEGF groups. The liver/brain ratio (that is, the relative liver mass) of the CHO-VEGF group (4.73 ± 0.39) was significantly increased compared with that of the CHO–dihydrofolate reductase (CHO-DHFR) (3.18 ± 0.25; $P < 0.0001$) and CHO–Hakata antigen (CHO-HAg) (3.00 ± 0.45; $P < 0.0001$) controls. This reflects an increase in relative liver masses of 49% and 59%, respectively.

Histological analysis of the livers of

Departments of [1]Molecular Oncology, [2]Protein Engineering, and [3]Pathology, Genentech Inc., 1 DNA Way, South San Francisco, CA 94080, USA.

*Present address: Amgen, Alpenquai 30, Post Office Box 2065, CH-6002 Lucerne, Switzerland.
†To whom correspondence should be addressed. E-mail: nf@gene.com

Myc-Induced T Cell Leukemia in Transgenic Zebrafish

David M. Langenau *et al.*

Science **299**, 887 (2003);
DOI: 10.1126/science.1080280

Science (print ISSN 0036-8075; online ISSN 1095-9203) is published weekly, except the last week in December, by the American Association for the Advancement of Science, 1200 New York Avenue NW, Washington, DC 20005.